



HAL
open science

Modeling of the Degradation of Elastic Properties due to the Evolution of Ductile Damage

Mathias Wallin, Mattias Olsson, Matti Ristinmaa

► **To cite this version:**

Mathias Wallin, Mattias Olsson, Matti Ristinmaa. Modeling of the Degradation of Elastic Properties due to the Evolution of Ductile Damage. *International Journal of Damage Mechanics*, 2008, 17 (2), pp.149-172. 10.1177/1056789506069468 . hal-00571163

HAL Id: hal-00571163

<https://hal.science/hal-00571163>

Submitted on 1 Mar 2011

HAL is a multi-disciplinary open access archive for the deposit and dissemination of scientific research documents, whether they are published or not. The documents may come from teaching and research institutions in France or abroad, or from public or private research centers.

L'archive ouverte pluridisciplinaire **HAL**, est destinée au dépôt et à la diffusion de documents scientifiques de niveau recherche, publiés ou non, émanant des établissements d'enseignement et de recherche français ou étrangers, des laboratoires publics ou privés.

Modeling of the Degradation of Elastic Properties due to the Evolution of Ductile Damage

MATHIAS WALLIN,* MATTIAS OLSSON AND MATTI RISTINMAA
*Division of Solid Mechanics, Lund University, P.O. Box 118
SE-22100 Lund, Sweden*

ABSTRACT: An elasto-plastic constitutive model for porous materials is formulated within the thermodynamic framework. The formulation facilitates a natural modeling of damage as well as growth and the shrinkage of voids. Metal plasticity is used for demonstrating the possibilities of the formulation. The yield function employed is assumed to depend upon the void-volume fraction, whereas the free energy is dependent on a scalar damage field. To show the capabilities of the model the algorithmic constitutive equations are derived and implemented into a finite element program. It is shown that an extremely simple system involving only two scalar equations needs to be solved in the constitutive driver. Two numerical examples are considered: the necking of an axi-symmetric bar and localization in a notched specimen.

KEY WORDS: ductile void growth, damage mechanics, thermodynamics.

INTRODUCTION

IF A CONTINUOUSLY increasing load is applied to a structure, this obviously leads to failure of the structure. In metals, the failure is to a high degree governed by the growth and nucleation of voids or pores and by the formation of microcracks. A large number of experimental studies of the mechanisms governing the kinematics of pores in metals have been published, e.g., Hancock and Mackenzie (1976) for an investigation of structural steel. It has been found that pores can originate from

*Author to whom correspondence should be addressed. E-mail: Mathias.Wallin@solid.lth.se

second-phase inclusions in the material, such parameters as size, stiffness, and orientation of the particles have been found to influence the nucleation process. The coalescence of neighboring voids is another important mechanism which plays an important role in the deformation process in metals at moderate to large levels of void density.

The evolution of voids is usually modeled by introducing an additional scalar field which represents the void-volume fraction. Two factors are assumed to contribute to the evolution of the porosity, or of the void-volume fraction, one of them accounting for the growth of existing voids and the other being concerned with the nucleation of the voids. Void growth is assumed to be driven by the hydrostatic pressure and it is usually modeled by the evolution law proposed by Gurson (1977). The rate of nucleation of voids is due to decohesion at the particle–matrix interface at second phase material inclusions and is usually assumed to consist of one part dependent upon the rate of change of the yield stress of the matrix material and of another part dependent upon the hydrostatic pressure (Needleman and Rice, 1978).

The frequently employed pressure-sensitive yield criterion proposed by Gurson (1977) is micromechanical-based and it is obtained from an upper-bound solution to the situation in which a void is present in an incompressible rigid–plastic matrix. Gurson’s model was later modified by Tvergaard (1988) to improve its predictive capabilities for low void-volume fractions. Brown and Embury (1973), on the basis of experiments and of a model for local necking showed that a significant degree of coalescence of voids occurs at some threshold value of the void-volume fraction. This phenomena was originally incorporated into the Gurson model by Tvergaard and Needleman (1984). In the present study, an alternative yield function is employed (Olsson, 2003). Both of the yield conditions aforescribed allow for growth and shrinkage of the voids. This is in contrast to the phenomenological model proposed by Rousselier (1987), which only allows increase in the void-volume fraction. Despite that formulations for the anisotropic growth of voids exist (Benzerga et al., 2002; Wang et al., 2004; Lassance et al., 2006), the present study is restricted, for the sake of simplicity, to isotropic void growth.

In addition to the influence of the void-volume ratio authors consider the degradation of the free energy within the classical damage framework (Lemaitre and Chaboche, 1990; Kachanov, 1958). In general, when considering anisotropic damage higher order tensors must be introduced in the formulation (Menzel et al., 2005). Here, we will restrict ourself to isotropic damage and consequently a scalar damage field is sufficient. The scalar-valued damage field is introduced in Helmholtz’s free energy which allows the elastic properties to naturally depend upon the

damage accumulation. In the present formulation the evolution of damage is governed by the void-volume evolution. In fact, the damage accumulation is taken as the maximum void-volume fraction during the loading process. This coupling effect (damage accumulation–void growth), normally ignored in micromechanics-based formulations, is taken into account for the present study.

In micromechanics based models of porous materials in which there is isotropic hardening, the postulate of equivalent plastic power is commonly adopted as the basis to form evolution law for isotropic hardening. This contrasts with thermodynamically based plasticity theories, in which common use is made of the postulate of maximum dissipation, which leads to the so-called associated evolution laws (Ottosen and Ristinmaa, 2005). In the present work, both the associated evolution laws for plastic flow and the variables associated with isotropic hardening are adopted. It is shown that the balance of plastic power at both a microscopic and a macroscopic level is recovered as a special case.

The algorithmic development of constitutive models in which void growth and damage evolution are included has been considered earlier by, e.g., Aravas (1987), Mahnken (1999), Mahnken (2002), Kojic et al. (2002), and Mühlich and Brocks (2003). Usually an implicit backward Euler approximation and/or an exponential update (Weber and Anand, 1990) is applied to the constitutive equations, along with requiring that the yield criterion is fulfilled at the end of the integration interval. This approach needs to be used with care, however, since it has been shown (Wallin and Ristinmaa, 2001), that damage evolution is very sensitive to the step-size. In the present study, the exponential update is applied to the evolution law for plastic flow, whereas the backward Euler scheme is applied to the isotropic hardening evolution law. The efficiency of the integration procedure is increased by making use of the coaxiality of the elastic deformation and the gradient of the yield function.

PRELIMINARIES

Let $\Omega_0 \subset \mathbb{R}^3$ denote the body in the reference configuration and let particles in the reference configuration be identified by their position vector \mathbf{X} . The motion of the particles is described by the nonlinear mapping $\varphi: \Omega_0 \times T \rightarrow \Omega \subset \mathbb{R}^3$, where T denotes the time interval and Ω defines the body in the deformed configuration. The linear mapping defined by the deformation gradient $\mathbf{F} = \varphi \otimes \nabla_{\mathbf{X}}$, describes the local deformation of the body. The Jacobian is defined as $J = \det \mathbf{F} = \rho_0 / \rho > 0$, where ρ_0 and ρ are the densities in the reference and current configuration, respectively.

To introduce plasticity, the multiplicative split of the deformation gradient is adopted,

$$\mathbf{F} = \mathbf{F}^e \mathbf{F}^p \quad (1)$$

where \mathbf{F}^e and \mathbf{F}^p define, respectively, the elastic and plastic contributions of the total deformation gradient (Kröner, 1960; Lee, 1969). For metal plasticity, \mathbf{F}^e describes the reversible distortion of the crystal lattice whereas \mathbf{F}^p describes the irreversible deformation of it. J^e and J^p are defined, in a similar manner to J as $J^e = \det \mathbf{F}^e$ and $J^p = \det \mathbf{F}^p$, respectively. To simplify the derivations it will be assumed that the intermediate configuration is isoclinic. For later use, it is noted that the split of the deformation gradient in Equation (1) provides the following kinematic relation

$$\mathbf{L} = \dot{\mathbf{F}}\mathbf{F}^{-1} = \mathbf{l}^e + \mathbf{F}^e \mathbf{l}^p \mathbf{F}^{e-1} \quad (2)$$

where \mathbf{L} is the spatial velocity gradient and where both $\mathbf{l}^e = \dot{\mathbf{F}}^e \mathbf{F}^{e-1}$ and $\mathbf{l}^p = \dot{\mathbf{F}}^p \mathbf{F}^{p-1}$ are introduced. Moreover, for later purposes the symmetric part of \mathbf{L} is introduced as the rate of deformation tensor, i.e., $\mathbf{D} = \text{sym}(\mathbf{L})$.

For metals, the concept of plasticity includes such irreversible phenomena as generation and movements of dislocations as well as nucleation and the growth of voids and microcracks. The generation and movement of dislocations are traditionally modeled as an isochoric process whereas the process of void-volume growth obviously involves a change of volume. The present study is restricted to isotropic void-volume growth and nucleation, the voids being assumed, to be spherical in shape and to be uniformly distributed, allowing them to be described by a single scalar J^v . The variable, J^v is defined as the volume change due to the voids present in a matrix material. Formally, we introduce J^v by considering a representative volume element (RVE) and defining it as the ratio of the total volume v to the RVE and the volume occupied by the matrix material v_m , where the volume of the RVE is decomposed into $v = v_m + v_v$, where v_v is obviously the volume occupied by the voids. It then follows that

$$J^v = \frac{v}{v_m} \quad (3)$$

The porosity f of the porous materials or the void-volume fraction, as is usually employed in constitutive descriptions, is defined as

$$f = \frac{v_v}{v} \quad (4)$$

which can be related to J^v as

$$f = 1 - \frac{1}{J^v} \quad (5)$$

The evolution of voids is usually assumed to be a contribution of two different mechanisms; namely, the growth of existing voids and the nucleation of voids, or the formation of new voids from existing inclusions. Thus, the evolution law of J^v could be written formally as

$$\overline{\dot{\ln J^v}} = \overline{(\dot{\ln J^v})}_{\text{growth}} + \overline{(\dot{\ln J^v})}_{\text{nucleation}} \quad (6)$$

where the first term on the right-hand side is due to growth and the second term is present when the threshold for the nucleation of a new void has been reached. To simplify the presentation, only the growth of existing voids will be considered.

Taking advantage of the fact that the Jacobian J is defined as the fraction of the volume in the deformed configuration and of the volume in the reference configuration, i.e., $J = v/v_0$, where v_0 is the total volume in the reference configuration of the RVE, allows for a very useful interpretation of the damage variable J^v to be derived. Using the relationship $J = J^e J^p$, which follows from Equation (1), and that $J = v/v_0$ it can be concluded that

$$\overline{\dot{\ln J}} = \frac{\dot{v}}{v} = \overline{\dot{\ln J^e}} + \overline{\dot{\ln J^p}} \quad (7)$$

However, from Equations (3) and (5) it follows that

$$\overline{\dot{\ln J^v}} = \dot{J}^v / J^v = \frac{\dot{v}}{v} - \frac{\dot{v}_m}{v_m} = \frac{\dot{f}}{1-f} \quad (8)$$

which allows the important relation

$$\overline{\dot{\ln J^v}} = \overline{\dot{\ln J^e}} + \overline{\dot{\ln J^p}} - \frac{\dot{v}_m}{v_m} \quad (9)$$

to be established. Generally, v_m develops both for elastic and plastic response. It will be assumed here that the matrix material is plastically incompressible, so that v_m is dependent upon the elastic response only. By assuming that void growth is due only to plasticity, it can be concluded that

$$\overline{\dot{\ln J^e}} = \dot{v}_m / v_m$$

holds, and also that

$$\overline{\dot{\ln J^v}} = \overline{\dot{\ln J^p}} = \text{tr}(\mathbf{I}^p) \quad (10)$$

where the operator tr denotes the trace of a second-order tensor. The second equality in Equation (10) is found by applying Liouville's theorem to \mathbf{F}^p . The well-known expression for the evolution law for the void-volume fraction is obtained if advantage of Equation (8) is taken, i.e.,

$$\dot{f} = (1 - f)tr(\mathbf{I}^p) \quad (11)$$

is obtained. The format (11) is the evolution law for void growth that Gurson (1975) proposed. The evolution law just mentioned is redundant in the present formulation, however, and need not to be considered when the constitutive model is established, a conclusion which follows from the fact that an integration of Equation (10) is possible, yielding

$$J^v = J^{v_0} J^p \quad (12)$$

where J^{v_0} is due to voids present in the reference configuration. Thus, knowledge of J^p allows J^v or f to be calculated explicitly via Equation (5). This will be used later when the evolution laws are established.

In addition to the void-volume ratio given by f (or J_v) an additional scalar field α representing the damage accumulation is introduced in the model. The motivation for introducing the field α different from the void-volume fraction f is to memorize the largest volume of void-volume ratio.

Thermodynamics

An admissible thermodynamic process is defined as one which satisfies the postulate of the conservation of energy (first law of thermodynamics) and the postulate of the growth of entropy (second law of thermodynamics) (Truesdell and Toupin, 1960). The second law of thermodynamics, which places restrictions on the model, can be reduced to the dissipation inequality

$$\gamma_0 = \boldsymbol{\tau} : \mathbf{D} - \frac{J}{\theta} \mathbf{q} \cdot \nabla_x \theta - \rho_0 \dot{\psi} \geq 0 \quad (13)$$

where the Kirchhoff stress $\boldsymbol{\tau}$ is related to the Cauchy stress via $\boldsymbol{\tau} = J\boldsymbol{\sigma}$. The temperature and heat flux vector are denoted as θ and \mathbf{q} , respectively. In the elasto-plastic model considered here, both isotropic hardening and elastic degradation is considered. Assuming isothermal conditions, it is postulated that Helmholtz's free energy can be written as $\psi(\mathbf{C}^e, \varepsilon_m^p, \alpha)$, where $\mathbf{C}^e = \mathbf{F}^{eT} \mathbf{F}^e$ is the elastic deformation tensor and ε_m^p is the internal variable associated with isotropic hardening in the model. The internal variable α

is associated with the elastic degradation due to damage and in the present formulation an isotropic damage dependence is utilized. If other effects are considered, additional internal variables need to be introduced into Helmholtz's free energy. For present purposes, however, the earlier format is sufficient. Inserting Helmholtz's free energy into the dissipation inequality (13) and taking advantage of Equation (2) results in

$$\gamma_0 = \left(\boldsymbol{\tau} - 2\rho_0 \mathbf{F}^e \frac{\partial \psi}{\partial \mathbf{C}^e} \mathbf{F}^{eT} \right) : \mathbf{D} + S^d \dot{\alpha} + \boldsymbol{\Sigma} : \mathbf{I}^p - R \dot{\varepsilon}_m^p - \frac{J}{\theta} \mathbf{q} \cdot \nabla_x \theta \geq 0 \quad (14)$$

where the Mandel stress tensor, $\boldsymbol{\Sigma}$, and the thermodynamic force, R , conjugated to $\dot{\varepsilon}_m^p$ and damage stress S^d were introduced as

$$\boldsymbol{\Sigma} = 2\rho_0 \mathbf{C}^e \frac{\partial \psi}{\partial \mathbf{C}^e}, \quad R = \rho_0 \frac{\partial \psi}{\partial \varepsilon_m^p} \quad \text{and} \quad S^d = -\rho_0 \frac{\partial \psi}{\partial \alpha} \quad (15)$$

One allowable solution is given by the following constitutive relations for the Kirchhoff stress

$$\boldsymbol{\tau} = 2\rho_0 \mathbf{F}^e \frac{\partial \psi}{\partial \mathbf{C}^e} \mathbf{F}^{eT} \quad (16)$$

which allows the dissipation inequality (14) to be reduced to

$$\gamma_0 = \boldsymbol{\Sigma} : \mathbf{I}^p + S^d \dot{\alpha} - R \dot{\varepsilon}_m^p - \frac{J}{\theta} \mathbf{q} \cdot \nabla_x \theta \geq 0 \quad (17)$$

A conservative approach to fulfill the second law is to split of the dissipation inequality (17) into

$$\gamma_0^{(1)} = \boldsymbol{\Sigma} : \mathbf{I}^p - R \dot{\varepsilon}_m^p \geq 0, \quad \gamma_0^{(2)} = S^d \dot{\alpha} \geq 0, \quad \gamma_0^{\text{therm}} = -\frac{J}{\theta} \mathbf{q} \cdot \nabla_x \theta \quad (18)$$

that means $\gamma_0^{(1)} \geq 0$, $\gamma_0^{(2)} \geq 0$ and $\gamma_0^{\text{therm}} \geq 0$ are fulfilled independently. Moreover, since no thermal coupling effects will be considered it will be assumed that $\gamma_0^{\text{therm}} \geq 0$.

In order to establish proper evolution laws for \mathbf{I}^p and $\dot{\varepsilon}_m^p$, the first part of the dissipation inequality (18) needs to be considered. Associated plasticity will be adopted here and a convex yield function $F(\boldsymbol{\Sigma}, R; J^v) \leq 0$ defining the elastic region is introduced. Note that J^v is considered as being a parameter in F . To ensure that $\gamma_0^{(1)} \geq 0$ we adopt the postulate of maximum dissipation which can be formulated as a minimization problem by introducing the Lagrangian $\mathcal{L} = -\gamma_0^{(1)} + \lambda F$. The Lagrangian multiplier is denoted as λ .

For given fluxes I^p and $\dot{\epsilon}_m^p$ as well as J^v , stationarity with respect to the Mandel stress Σ and R of the Lagrangian functional \mathcal{L} , provide the following evolution laws:

$$I^p = \lambda \frac{\partial F}{\partial \Sigma} \quad \text{and} \quad \dot{\epsilon}_m^p = -\lambda \frac{\partial F}{\partial R} \quad (19)$$

Note that in the present formulation the evolution of the void-volume, cf. Equations (10) and (12), is given implicitly by the evolution law (19a).

The plastic multiplier λ is determined from the Kuhn–Tucker conditions, which also follow from the minimization procedure

$$\lambda \geq 0, \quad F\lambda = 0, \quad \text{and} \quad F \leq 0 \quad (20)$$

From the conditions in Equation (20), it follows that plastic loading can take place only when $F=0$. For plastic loading to continue, it is required that $\dot{F}=0$ hold. The relation $\dot{F}=0$ is known as the consistency relation.

When considering elasto-plastic constitutive models coupled with damage, one important question is how to establish the evolution law for the damage variable. A possible form for the evolution of the damage is to associate the damage to the evolution of the void-volume ratio. Here, we will use α to memorize the most severe loading conditions, that is the largest value of the void-volume ratio. Thus, it turns out that a natural choice for the evolution of α is given by

$$\dot{\alpha} = \begin{cases} \dot{f} & \text{if } \alpha = f \quad \text{and} \quad \dot{f} > 0 \\ 0 & \text{otherwise} \end{cases} \quad (21)$$

i.e., the damage field α is defined by the maximum void volume during the loading process. From Equation (21) it follows that α is an internal variable that memorizes the maximum void-volume ratio. Evidently, more refined suggestions for $\dot{\alpha}$ can be proposed, however, the format (21) suffices for the present purposes. To proceed, let us turn to the stress conjugated to α , i.e., S^d . Instinctively, we expect that the stiffness and the hardening of the material will decrease with increasing damage which indicates that S^d is positive, cf. Equation (15). In the following discussion, we will consequently assume that $S^d > 0$, which along with Equation (21) reveals that $\gamma_0^{(2)} \geq 0$.

Remark: Note that for the situation where no decrease in void growth takes place the proposed evolution law (21) will imply that the void-volume ratio equals the damage, i.e., $\alpha = f$.

SPECIFIC CONSTITUTIVE MODEL

Assuming isotropic elasticity and isotropic plastic hardening, Helmholtz's free energy is chosen as

$$\rho_0 \psi(\mathbf{C}^e, \varepsilon_m^p, \alpha) = \frac{1}{2} K (I_1^e)^2 + 2GJ_2^e + R_\infty (\varepsilon_m^p + \varepsilon_0 \exp(-\varepsilon_m^p/\varepsilon_0)) + \frac{1}{2} H_\infty (\varepsilon_m^p)^2 \quad (22)$$

where R_∞ , H_∞ , and ε_0 are material parameters describing the hardening of the material. That damage accumulation is assumed to enter the free energy via the hardening parameters R_∞ and H_∞ , as well as the bulk modulus K and the shear modulus G . The two strain invariants I_1^e and J_2^e present in Equation (22) are defined as

$$I_1^e = \text{tr}(\ln \mathbf{U}^e) = \ln J^e \quad \text{and} \quad J_2^e = \frac{1}{2} [(\ln \mathbf{U}^e)^{\text{dev}} (\ln \mathbf{U}^e)^{\text{dev}}] \quad (23)$$

where the superscript dev denotes the deviatoric part of a second-order tensor. \mathbf{U}^e is the right elastic stretch tensor which follows from the polar decomposition of $\mathbf{F}^e = \mathbf{R}^e \mathbf{U}^e$. The Kirchhoff stress, cf. Equation (16), and the Mandel stress, cf. Equation (15a), both resulting from Equation (22), are given as

$$\boldsymbol{\tau} = K \ln J^e \mathbf{1} + 2G(\ln \mathbf{V}^e)^{\text{dev}} \quad \text{and} \quad \boldsymbol{\Sigma} = K \ln J^e \mathbf{1} + 2G(\ln \mathbf{U}^e)^{\text{dev}} \quad (24)$$

where \mathbf{V}^e is the left stretch tensor following from the polar decomposition $\mathbf{F}^e = \mathbf{V}^e \mathbf{R}^e$. Note that Helmholtz's free energy (22) gives rise to a natural isochoric–volumetric split of the elastic stress–strain relation. For completeness, it is noted that the thermodynamic force R conjugated to the effective plastic strain, ε_m^p , becomes

$$R = R_\infty (1 - \exp(-\varepsilon_m^p/\varepsilon_0)) + H_\infty \varepsilon_m^p \quad (25)$$

Using the results of Budiansky (1970), and following Davison et al. (1977) and Rabier (1989), a model can be found, in which the bulk modulus K and the shear modulus G depend on the damage. For a composite with two constituents, one of which is the collection of voids, the voids being associated both with a zero shear modulus and a zero bulk modulus, it follows that

$$\begin{aligned} K &= K_0 \left[1 - \frac{3(1 - \nu_0)}{2(1 - 2\nu_0)} \alpha \right] \\ G &= G_0 \left[1 - \frac{15(1 - \nu_0)}{7 - 5\nu_0} \alpha \right] \end{aligned} \quad (26)$$

where K_o , G_o , and ν_o are the bulk modulus, the shear modulus, and Poisson's ratio, respectively, for the virgin material. In analogy to the elastic parameters, it is natural to assume that both R_∞ and H_∞ depend on α (Olsson and Ristinmaa, 2003). Since no explicit expressions of their dependencies on the damage can be found in the literature, it is will conveniently be assumed that

$$R_\infty = R_\infty^m(1 - h(\alpha)), \quad H_\infty = H_\infty^m(1 - h(\alpha)) \quad (27)$$

where R_∞^m will be identified later as the saturation of the exponential part of the hardening of the matrix material and H_∞^m as the asymptotic hardening modulus of the matrix material for large values of ε_m^p . The function $h(\alpha)$ describing the dependency on the void-volume fraction, will be considered later on.

Remark: It was previously assumed that $S^d > 0$. For the present model it can easily be shown that $S^d = -\rho_0(\partial\psi/\partial\alpha) > 0$ if $h'(\alpha) > 0$.

In Olsson (2003) a yield function for porous materials was proposed. This yield function by Tvergaard (1981) and Tvergaard and Needleman (1984), together with modifications, similar to those introduced for Gurson's (1977) yield function, will be adopted here. The format of the yield function is given as

$$F = B \left(\Sigma_e^2 + \left(\frac{1(1 - q_1 f^*(f)) q_2 \Sigma_t}{2 \ln(q_1 f^*(f))} \right)^2 - ((1 - q_1 f^*(f)) \sigma_m)^2 \right) \quad (28)$$

where $B = (1 - q_1 f^*(\alpha)) / (2(1 - q_1 f^*(f))^2 \sigma_m)$. Moreover, σ_m denotes the yield stress for the matrix material, $\Sigma_e = ((3/2) \Sigma^{\text{dev}} : \Sigma^{\text{dev}})^{1/2}$ and $\Sigma_t = \text{tr}(\Sigma)$. The material parameters q_1 and q_2 present in Equation (28) are similar to the parameters introduced by Tvergaard (1981) to improve the Gurson model for low void-volume fractions. The function $f^*(f)$ taken from Tvergaard and Needleman (1984) is defined as

$$f^*(f) = \begin{cases} f & \text{for } f \leq f_c \\ f_c + \frac{f_u^* - f_c}{f_f - f_c} (f - f_c) & \text{for } f > f_c \end{cases} \quad (29)$$

This function is so adjusted that zero stress is obtained when $f^* = f_u^* = 1/q_1$, complete loss of stress-carrying capacity thus being obtained for $f \rightarrow f_f$. On the basis of experiments and a simple model for local necking,

Brown and Embury (1973) found the void-volume fraction at coalescence to be $f_c \approx 0.15$ and the analysis by Andersson (1977) showed that the void-volume fraction at fracture is approximately 0.25. The reason for introducing the scaling B is that a simple interpretation of the plastic multiplier is obtained. Note also that since $(1 - q_1 f^*(f))/\ln(q_1 f^*(f)) \rightarrow 0$ as $f \rightarrow 0$, Equation (28) degenerates in the case of no voids being present, to the usual von Mises criterion. To obtain a yield stress of the (damage free) matrix material, that does not depend on the damage accumulation, the following form is chosen

$$\sigma_m = \sigma_{y0} + R(\varepsilon_m^p, \alpha)/(1 - h(\alpha)) \quad (30)$$

where σ_{y0} denotes the initial yield stress of the matrix material. Accordingly, use of Equations (25) and (27) enables the yield stress of the matrix material to be identified as

$$\sigma_m = \sigma_{y0} + R_\infty^m (1 - \exp(-\varepsilon_m^p/\varepsilon_0)) + H_\infty^m \varepsilon_m^p = \sigma_m(\varepsilon_m^p) \quad (31)$$

which clearly shows the yield stress of the matrix material, σ_m , as previously stated, is independent of the damage. For simplicity, it will also be assumed that $h(z) = q_1 f^*(z)$, since this yields a natural format for the mechanical dissipation. The present model does not consider the size and location of the individual pores, i.e., the formulation does not involve a length scale. In order to take that effect into account, Håkansson et al. (2006) introduced a smeared void-volume ratio and consequently a length scale into the Gurson formulation. This approach does, however, introduce an additional boundary value problem and will for simplicity not be utilized in the present formulation.

The implications of the proposed model will now be considered. Taking advantage of Equations (20b), (28), and (30) results in the following expression for the rate of effective plastic strain:

$$\dot{\varepsilon}_m^p = \lambda \quad (32)$$

Straightforward derivation using Equations (19), (28), and (32) results in

$$\Sigma : \mathbf{I}^p = (1 - q_1 f^*(\alpha)) \sigma_m \dot{\varepsilon}_m^p \quad (33)$$

Note that for the situation where $q_1 = 1$ and $f = \alpha$, Equation (33) reduces $\Sigma : \mathbf{I}^p = (1 - f) \sigma_m \dot{\varepsilon}_m^p$ which usually is adopted as the basis to form the evolution laws for $\dot{\varepsilon}_m^p$.

Finally, the explicit format for the dissipation shown in Equation (17) will be investigated. Using the results shown in Equations (32) and (33) one can express the dissipation as

$$\gamma_0^{(1)} = \Sigma : \mathbf{I}^p - R\dot{\varepsilon}_m^p = \lambda(1 - q_1 f^*(\alpha))\sigma_{y0} \quad (34)$$

From Equation (34), one can conclude that the dissipation inequality is clearly fulfilled. Moreover, since $\gamma_0^{(2)}$ vanish for the situation where $\dot{\alpha} = 0$, it follows that for the situation $\alpha \equiv 0$, the mechanical dissipation degenerates to the dissipation resulting from an associated isotropic hardening von Mises formulation.

NUMERICAL TREATMENT

In order to make use of path-dependent constitutive models in a finite element context, numerical algorithms for the integration of the constitutive equations must be employed. Use of an implicit finite element formulation also requires establishment of the algorithmic tangent-stiffness tensor. Thus, a consistent linearization of the integration algorithm is necessary if the quadratic convergence rate in the equilibrium iterations is to be preserved. In the present study, an implicit integration algorithm based on the exponential map (Weber and Anand, 1990) and the backward Euler scheme is applied to the constitutive equations. To increase the efficiency of the integration procedure, a spectral decomposition of the constitutive equations is employed.

Integration Scheme

Before entering the discussion regarding the updating of the state variables, a check on whether plastic evolution has taken place during the load increment is needed. The trial quantities used to determine whether elastic or plastic response has taken place are obtained from an assumed purely elastic response:

$$\mathbf{F}^{e,tr} = \mathbf{F}^{n+1}(\mathbf{F}^{p,n})^{-1}, \quad \varepsilon_m^{p,tr} = \varepsilon_m^{p,n}, \quad f^{tr} = f^n, \quad \alpha^{tr} = \alpha^n \quad (35)$$

where the superscripts tr and n refer to quantities in the trial state and in the last accepted equilibrium state, respectively. For elastic loading, i.e., where $\mathbf{F}(\Sigma(\mathbf{F}^{e,tr}, \alpha^{tr}), R(\varepsilon_m^{p,tr}, \alpha^{tr}), f^{tr}) \leq 0$, the trial quantities are accepted as the updated state. For the case, however in which, $\mathbf{F}(\Sigma(\mathbf{F}^{e,tr}, \alpha^{tr}), R(\varepsilon_m^{p,tr}, \alpha^{tr}), f^{tr}) > 0$, plastic response has taken place. In addition to this

standard trial state we have to investigate the algorithmic counterpart to Equation (21). For the situation where $\alpha^n = f^n$ and $\text{tr}(\Sigma^{tr}) > 0$ we use that $\alpha^{n+1} = f^{n+1}$ whereas $\alpha^{n+1} = \alpha^n$ otherwise. The internal variables are then updated using an exponential update for F^p and a backward-Euler update for ε_m^p , such that

$$\begin{aligned} F^p &= \exp(\Delta\lambda\partial_{\Sigma}F)F^{p,n} = A^p F^{p,n}, \\ \varepsilon_m^p &= \varepsilon_m^{p,n} - \Delta\lambda\partial_R F, \\ F(\Sigma(C^e, \alpha), R(\varepsilon_m^p, \alpha), f) &= 0 \end{aligned} \quad (36)$$

a system of non-linear equations is to be solved. To simplify the notation, the superscript $n+1$ was dropped in Equation (36). Note that although α is present in Equation (36) no extra algebraic equation needs to be solved. To proceed it will be assumed that $\alpha = f$, i.e., $\dot{\alpha} = \dot{f}$. The situation $\dot{\alpha} = 0$ is found by taking $\alpha = \alpha^{tr}$ in the following derivations.

Due to the symmetry of C^e , the dimension of the system (37) can be reduced if the following equations are considered

$$\begin{aligned} \mathcal{R}_{C^e} &= C^e - A^{p-T} C^{e,tr} A^{p-1} \\ \mathcal{R}_{\varepsilon_m^p} &= \varepsilon_m^p - \varepsilon_m^{p,tr} + \Delta\lambda\partial_R F \\ \mathcal{R}_F &= F(\Sigma(C^e, f), R(\varepsilon_m^p, f), f) \end{aligned} \quad (37)$$

in which $C^{e,tr} = F^{e,tr,T} F^{e,tr}$ is introduced. Note that the updated state $Y = [C^e, \varepsilon_m^p, \Delta\lambda]$ can be obtained by a direct solution of Equation (37) (i.e., $\mathcal{R} = [\mathcal{R}_{C^e}, \mathcal{R}_{\varepsilon_m^p}, \mathcal{R}_F] = 0$); this approach is not employed here, however, a further reduction of the system (37) being carried out instead.

In order to investigate whether the algorithm can be simplified, the coaxiality of the terms involved in Equation (37a) is considered. For the case in which $F = F(\Sigma_e, \Sigma_t, R, f)$, the plastic flow direction can be expressed as

$$\partial_{\Sigma}F = \frac{3G}{\Sigma_e} \frac{\partial F}{\partial \Sigma_e} \ln U_i^e + \frac{\partial F}{\partial \Sigma_t} \mathbf{1} \quad (38)$$

where the subscript i denotes the isochoric part of the tensor in question. Using the spectral decomposition $\ln U_i^e = \sum_{\alpha} \ln \lambda_i^{e,\alpha} \mathbf{n}^{\alpha} \otimes \mathbf{n}^{\alpha}$ it follows from Equation (38) that $\partial_{\Sigma}F$ is coaxial to C^e and is thus also coaxial to $\exp(-\Delta\lambda\partial_{\Sigma}F)$. From Equation (37a) it can then be concluded that all of the components of Equation (37a) are coaxial to C^e (or $C^{e,tr}$).

Therefore, since $\mathbf{C}^{e, tr}$ is fixed during the solution process, only one eigenvalue problem needs to be solved.

Using the yield function in Equation (28), the plastic flow direction can be expressed as

$$\partial_{\Sigma} F = \sum_{\alpha} g^{\alpha} \mathbf{n}^{\alpha} \otimes \mathbf{n}^{\alpha}, \quad g^{\alpha} = 2B \left(3G \ln \lambda_i^{e, \alpha} + \frac{1}{4} \frac{(1 - q_1 f^*)^2 q_2^2 \Sigma_t}{(\ln(q_1 f^*))^2} \right) \quad (39)$$

The results provided by Simo and Taylor (1991) allow the eigenvalue basis $\mathbf{n}^{\alpha} \otimes \mathbf{n}^{\alpha}$ to be expressed in terms of $\mathbf{C}^{e, tr}$ and invariants of $\mathbf{C}^{e, tr}$. In the case in which coinciding eigenvalues are present, a perturbation of the eigenvalues is performed.

From the isochoric/volumetric split of Equation (37a), it follows that J^e is related to $J^{e, tr} = \det(\mathbf{F}^{e, tr})$ in the following manner:

$$J^e = J^{e, tr} \exp \left(-\Delta\lambda \sum_{\alpha} g^{\alpha} \right) = \exp \left(-\frac{3}{2} \Delta\lambda B \frac{(1 - q_1 f^*)^2 q_2^2 \Sigma_t}{(\ln(q_1 f^*))^2} \right) J^{e, tr} \quad (40)$$

where $\sum_{\alpha} \ln \lambda_i^{e, \alpha} = 0$ was used to obtain the second equality in Equation (40). The use of Equation (40) also enables Equation (37a) to be reduced to the simple format

$$\ln \lambda_i^{e, \alpha} (1 + 6BG\Delta\lambda) - \ln \lambda_i^{e, tr, \alpha} = 0 \quad (41)$$

Thus, the isochoric part of Equation (37) is given by Equation (41) and the volumetric part by Equation (40). Finally, by introducing the invariant $J_2^{e, tr} = (1/2) \sum_{\alpha} (\ln \lambda_i^{e, tr, \alpha})^2$ it follows that rather than solving Equations (37), (40) and using (41) in (37c) provide the following reduced system:

$$\begin{aligned} \mathcal{R}_1 &= J^e - \exp \left(-\frac{3}{2} \Delta\lambda B \frac{(1 - q_1 f^*)^2 q_2^2 \Sigma_t}{(\ln(q_1 f^*))^2} \right) J^{e, tr} \\ \mathcal{R}_2 &= \frac{12G^2 J_2^{e, tr}}{(1 + 6GB\Delta\lambda)^2} + \frac{1}{4} \frac{(1 - q_1 f^*)^2 (q_2 \Sigma_t)^2}{(\ln(q_1 f^*))^2} - (1 - q_1 f^*)^2 \sigma_m^2 \end{aligned} \quad (42)$$

where Equation (37b) obviously provides $\varepsilon_m^p = \varepsilon_m^{p, n} + \Delta\lambda$. A system of two equations and two unknowns ($\Delta\lambda, J^e$) is thus obtained. To summarize, once the solution to Equation (43) has been found, the state is trivially updated using Equations (39), (41), and (36). Note that in Equation (42), f (and α) is calculated using Equations (5), (12) and from the relation $J^p = J/J^e$.

The Newton–Raphson iteration scheme that is used to obtain the updated solution is simply given as

$$\mathbf{Y}^{i+1} = \mathbf{Y}^i - \left[\frac{\partial \mathcal{R}}{\partial \mathbf{Y}} \right]^i \mathcal{R}^i \quad (43)$$

where \mathbf{Y} is defined as $\mathbf{Y} = [J^e \ \Delta\lambda]$. Since calculation of the Jacobian $\partial_Y \mathcal{R}$, although straightforward, is lengthy, it will not be presented here.

ATS Tensor

The algorithmic tangent stiffness tensor, \mathcal{L} , that enters the consistent linearization of the equilibrium equations, is defined as

$$\mathcal{L} = 2 \frac{\partial \mathbf{S}}{\partial \mathbf{C}}, \quad \mathbf{S} = \mathbf{F}^{p-1} \mathbf{S}^e \mathbf{F}^{p-T}, \quad \mathbf{S}^e = 2\rho_0 \frac{\partial \psi}{\partial \mathbf{C}^e} \quad (44)$$

where \mathbf{S} and \mathbf{C} represent the second Piola–Kirchhoff stress tensor and the Cauchy–Green deformation tensor, respectively. Straightforward differentiation of Equation (44) leads to

$$\mathcal{L} = \mathbf{P} : \left(\frac{\partial \mathbf{S}^e}{\partial \mathbf{C}^e} : \frac{\partial \mathbf{C}^e}{\partial \mathbf{C}} + \frac{\partial \mathbf{S}^e}{\partial \alpha} \frac{\partial \alpha}{\partial \mathbf{C}} \right) + \mathbf{M} : \frac{\partial \mathbf{A}^{p-1}}{\partial \mathbf{C}} \quad (45)$$

where the Cartesian components of the fourth-order tensors \mathbf{P} and \mathbf{M} are defined as

$$P_{ijkl} = 2F_{ik}^{p-1} F_{jl}^{p-1}, \quad M_{ijkl} = 2 \left(F_{ik}^{p-1, n} S_{lt}^e F_{jt}^{p-1} + F_{it}^{p-1} S_{il}^e F_{jk}^{p-1, n} \right) \quad (46)$$

On the right-hand side in Equation (45), the terms $\partial_{\mathbf{C}^e} \mathbf{S}^e$ and $\partial \alpha \mathbf{S}^e$ within the parentheses follow from a direct differentiation using results provided by Miehe (1998). The remaining derivatives in Equation (45) are obtained from spectral representations of \mathbf{A}^p and \mathbf{C}^e , i.e., from

$$\mathbf{A}^p = \sum_{\alpha} \exp(\Delta\lambda g^{\alpha}) \mathbf{n}^{\alpha} \otimes \mathbf{n}^{\alpha} \quad \text{and} \quad \mathbf{C}^e = \sum_{\alpha} (\lambda^{e, \alpha})^2 \mathbf{n}^{\alpha} \otimes \mathbf{n}^{\alpha} \quad (47)$$

The derivatives of \mathbf{A}^{p-1} and \mathbf{C}^e can then be obtained as

$$d\mathbf{A}^{p-1} = \sum_{\alpha} d(\exp(-\Delta\lambda g^{\alpha})) \mathbf{n}^{\alpha} \otimes \mathbf{n}^{\alpha} + \exp(-\Delta\lambda g^{\alpha}) d(\mathbf{n}^{\alpha} \otimes \mathbf{n}^{\alpha}) \quad (48)$$

and

$$dC^e = \sum_{\alpha} d((\lambda^{e,\alpha})^2) \mathbf{n}^{\alpha} \otimes \mathbf{n}^{\alpha} + (\lambda^{e,\alpha})^2 d(\mathbf{n}^{\alpha} \otimes \mathbf{n}^{\alpha}) \quad (49)$$

respectively. From Equations (48) and (49) it follows that $\Delta\lambda$, $\lambda^{e,\alpha}$, g^{α} , and $\mathbf{n}^{\alpha} \otimes \mathbf{n}^{\alpha}$ need to be linearized. Some of the derivatives sought, however, are ones already implicitly calculated within the stress integration procedure and to realize this, consider the system Equation (42), which in fact can be written as

$$\mathcal{R}(Y(X^{tr}), X^{tr}) = \mathbf{0} \quad \forall X^{tr} \quad (50)$$

where $X^{tr} = [J^{e,tr} \quad J_2^{e,tr}]$ are the variables that drive the evolution of the internal variables. Differentiation of Equation (50) results in

$$\frac{\partial Y}{\partial X^{tr}} = - \left[\frac{\partial \mathcal{R}}{\partial Y} \right]^{-1} \frac{\partial \mathcal{R}}{\partial X^{tr}} \quad (51)$$

Since the derivative $\partial_{X^{tr}} \mathcal{R}$ is obtained from straightforward differentiation of Equation (42), and since $\partial_Y \mathcal{R}$ is used in the solution process in Equation (42), the important derivatives of J^e and $\Delta\lambda$ with respect to $J^{e,tr}$ and $J_2^{e,tr}$ are provided by Equation (51). For the remaining differentiations the reader is referred to the Appendix, where all the linearization found in Equation (45) can be obtained in a rather simple manner.

RESULTS

Two examples will be considered to illustrate the capabilities of the model. The parameters related to the elastic properties are given by

$$G_0 = 80.2 \text{ GPa}, \quad K_0 = 164.2 \text{ GPa}, \quad \nu_0 = 0.3$$

whereas the plastic behavior is governed by

$$\sigma_{y0} = 450 \text{ MPa}, \quad \varepsilon_0 = 59.1 \cdot 10^{-3}, \quad R_{\infty}^m = 265 \text{ MPa}, \quad H_{\infty}^m = 129.2 \text{ MPa}$$

The elastic and the plastic material data employed was taken from Wriggers et al. (1992). The material data related to the void growth was chosen in accordance with Tvergaard and Needleman (1984). The initial void-volume fraction is set to $f_0 = 0.005$ and the coefficients related to the modifications for low void-volume fraction are chosen as $q_1 = 1.5$ and $q_2 = 1$. Moreover, in accordance with $f_0 = 0.005$ we assume that the initial damage field is given by $\alpha_0 = f_0$. The parameters related to coalescence of the voids are chosen as

$$f_c = 0.15, \quad f_f = 0.25, \quad f_u^* = 1/q_1$$

The constitutive parameters given earlier characterize a typical steel and in order to fit the model to a experimental data use can be made of the optimization procedure by Springman and Kuna (2005).

The elements used in the numerical calculations are displacement based four-node quadrilaterals. It is well known that finite element simulations of damage-dependent materials result in mesh-dependent solutions in the final softening stage. To resolve this issue, gradient-enhanced formulations can be utilized (de Borst and Mühlhaus, 1992; de Borst et al., 1996; Svedberg and Runesson, 1997; Håkansson et al., 2006) or integral-enhanced formulations, (Bažant and Lin, 1988; Strömberg and Ristinmaa, 1996) neither of these approaches will be utilized here.

Necking of Circular Cylinder

The necking process of a cylindrical solid bar has previously been considered by Wriggers et al. (1992) and Simo and Miehe (1992) for example, in the context of thermo-plasticity and by Tvergaard and Needleman (1984), Becker and Needleman (1986), Aravas (1987) and Mahnken (2002) for porous materials. The finite element mesh used in the present simulation, as shown in Figure 1(a), consists of 750 axisymmetric elements. In order to

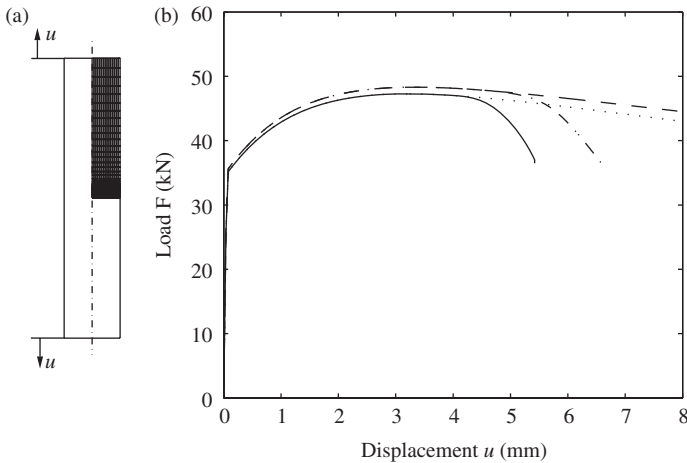


Figure 1. Necking of a cylindrical bar. (a) Geometry of the specimen and the finite element discretization and (b) The global response of a cylindrical bar subjected to a prescribed tensile load. The solid and the dotted lines represent the perturbated (nonhomogeneous) and the homogeneous solution, respectively, for the porous material. The dashed line and dashed-dotted line represent the homogeneous and the perturbated solution, respectively, for the matrix material.

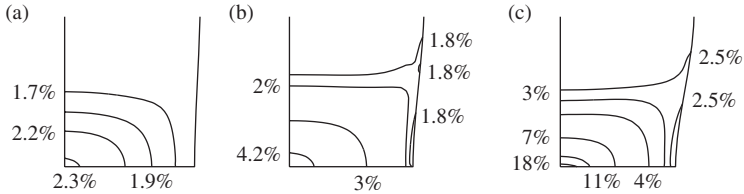


Figure 2. Evolution of damage α during a tensile test of a cylindrical bar. The void-volume-fraction distribution is shown for displacements at: (a) 4.8 mm, (b) 5.1 mm, and (c) 5.422 mm.

trigger the nonhomogeneous deformation mode, a small imperfection in the form of a radius reduction ($\Delta R/R = 0.0013$) is introduced. The bar is 50 mm in length and has a 5 mm radius.

Figure 1(b) shows the global force–displacement relation. The solid and the dotted line represent the perturbed and the homogeneous solution, respectively, for the porous material. The solution is terminated when the maximum porosity within the bar has reached $f_f = 0.25$, i.e., when in the most damaged region of the specimen no load carrying capacity is left. The perturbed solution shows a dramatic increase in porosity immediately after onset of the necking. For reference purposes, the response of a specimen consisting of pure matrix material ($f_0 = 0$, $\alpha_0 = 0$) is also shown in Figure 1(b). The homogeneous and the perturbed solutions for the matrix material are indicated by the dashed and the dashed-dotted lines, respectively. As expected (Becker and Needleman, 1986) the onset of necking takes place at a much later deformation stage for the matrix material than for the porous material.

Figure 2 shows the evolution of damage at different stages of the perturbed solution. As can be seen, the damage is greatest at the center of the specimen. This is due to the maximum hydrostatic pressure, which drives the growth of voids, being at a maximum at the center of the specimen. Although the solution process was continued to a stage at which $f = f_f$ was reached, the numerical algorithm turned out to be very stable, no numerical problems being encountered. Continuing the solution process requires an element-removal technique which is not implemented in the present work.

Localization in a Plane Strip

A plane strip subjected to a tensile load is considered, it is being assumed that plane strain conditions apply. The dimensions of the undeformed specimen are $s = 20$ mm, $w = 200$ mm, $v = 400$ mm, and $h = 400$ mm and the thickness is $t = 10$ mm, Figure 3(a), where the finite element mesh

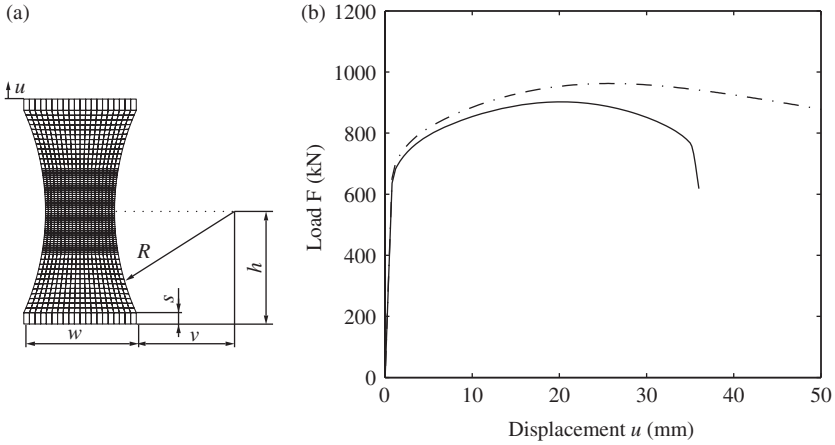


Figure 3. A tensile test of a notched specimen, plane strain conditions being assumed to prevail. (a) The initial geometry with an undeformed finite element mesh consisting of 1320 quadrilateral elements and (b) a load–displacement graph. The solid line represents the response of the porous material, whereas the response of the matrix material is indicated by the dashed–dotted line.

consisting of 1320 quadrilaterals is shown. Structures similar to the strip contained in Figure 3(a) have been considered previously by Benzerga et al. (2002) and Kojic et al. (2002). In Figure 3(b), the total applied force versus the displacement u is plotted. Please note that the specimen is free to move in the horizontal direction. At a displacement of $u=36$ mm the maximal void-volume fraction within the specimen has reached $f=f_f$, i.e., a crack has been created. Similar to the case of a cylindrical specimen, the crack is located at the center of the specimen where the hydrostatic pressure is at a maximum. Note for the porous material in Figure 4(b) the sharp drop in the load around $u=35$ mm, a drop caused by the diffuse necking that has taken place. No sharp drop of this sort could be detected for the situation $f=f_0=0$. Figure 4 shows the evolution of the void-volume fraction. During initial stages of the deformation, the isolines (of the void-volume fraction) are almost circular (Figure 4(a)). After the onset of necking, the isolines have become more rectangular in shape (Figure 4(c)). As in the simulation of the cylindrical specimen, the void-volume fraction $f=f_f$ was reached without numerical problems being encountered.

CONCLUSIONS

It was shown that a model for porous ductile fracture can be established within a consistent thermodynamic framework. A model that allows for

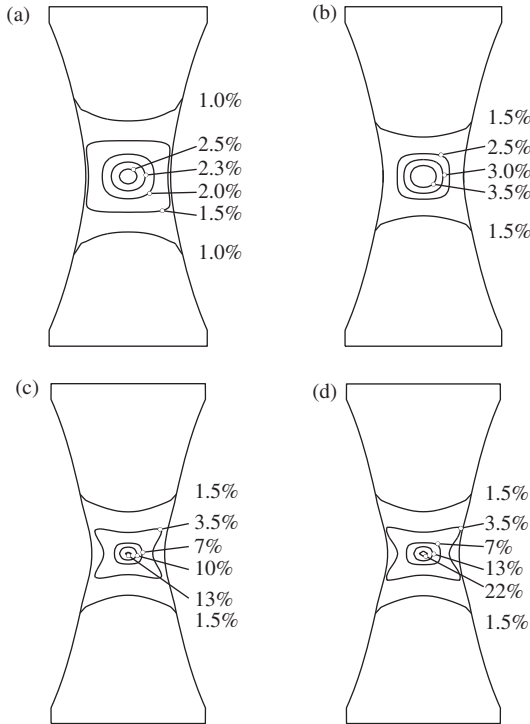


Figure 4. Evolution of the damage, α during the tensile test of a plane strip. The void-volume fraction distribution is shown for displacements: (a) 24 mm, (b) 28 mm, (c) 35 mm, and (d) 36 mm.

both growth and shrinkage of voids was considered within this framework. The model also accounts for isotropic damage which influences the response via both the usual elastic parameters and the parameters governing the plastic behavior. It could be shown that when the void-volume fraction equals zero the model degenerates into the usual von Mises plasticity model.

The model was implemented in a finite element program. It was found that, if the exponential update of \mathbf{F}^p was utilized, the constitutive relation took a very simple format, in fact, only two nonlinear equations needed to be solved. The algorithmic tangent stiffness tensor was also considered, and it was shown that it can easily be derived from the (two) reduced equations. It should be emphasized that no separate evolution equations for the void-volume fraction were needed, since it was shown that the void-volume fraction could be calculated explicitly from $J^p = \det(\mathbf{F}^p)$.

Two examples were considered as a final demonstration of the possibilities of the model involving an axi-symmetric bar and a plane

notched specimen, respectively. In both cases, the specimens were loaded up to the point at which somewhere in the material the stress-carrying capacity vanished indicating that the solution algorithm was very stable.

APPENDIX

It turns out that, to obtain the remaining derivatives contained in Equation (45), J , J^e , $\lambda^{e,tr}$, $\lambda_i^{e,tr}$, $J^{e,tr}$, $J_2^{e,tr}$, $\Delta\lambda$, and $\mathbf{n}^\alpha \otimes \mathbf{n}^\alpha$ need to be differentiated with respect to \mathbf{C} . Using Liouville's theorem, the linearization of J and $J^{e,tr}$ are obtained trivially as

$$d \ln J = d \ln J^{e,tr} = \frac{1}{2} \mathbf{C}^{-1} : d\mathbf{C} \quad (52)$$

where Equation (35) was used in the first equality. Following Simop and Taylor (1991) and using Equation (52), the linearization of the isochoric trial eigenvalues are obtained as

$$d \ln \lambda_i^{e,tr,\alpha} = \frac{1}{2} \left[N^\alpha \otimes N^\alpha - \frac{1}{3} \mathbf{C}^{-1} \right] : d\mathbf{C} \quad (53)$$

where the transformed eigenvectors N^α are defined as

$$N^\alpha = \frac{1}{\lambda^{e,tr,\alpha}} \mathbf{F}^{p,n,-1} \mathbf{n}^\alpha \quad (54)$$

and \mathbf{n}^α is an eigenvector belonging to $\mathbf{C}^{e,tr}$. Using the definition of $J_2^{e,tr}$, straightforward calculations with the use of Equation (53) result in

$$dJ_2^{e,tr} = \mathbf{Q} : d\mathbf{C}, \quad \text{where } \mathbf{Q} = \sum_\alpha (\ln \lambda_i^{e,tr,\alpha}) \frac{1}{2} [N^\alpha \otimes N^\alpha] \quad (55)$$

For notational simplicity, the scalars $a_1 - a_4$ are introduced as

$$a_1 = \frac{1}{2} \frac{J^{e,tr}}{J^e} \frac{\partial J^e}{\partial J^{e,tr}}, \quad a_2 = \frac{1}{J^e} \frac{\partial J^e}{\partial J_2^{e,tr}}, \quad a_3 = \frac{J^{e,tr}}{2} \frac{\partial \Delta\lambda}{\partial J^{e,tr}}, \quad a_4 = \frac{\partial \Delta\lambda}{\partial J_2^{e,tr}} \quad (56)$$

Use of Equation (56) enables the rate of change of $\ln J^e$ to be obtained as

$$d \ln J^e = [a_1 \mathbf{C}^{-1} + a_2 \mathbf{Q}] : d\mathbf{C} \quad (57)$$

In a similar way, just as for $\ln J^e$, the linearization of $\Delta\lambda$ and of ε_m^p are obtained as

$$d\Delta\lambda = d\varepsilon_m^p = [a_3 \mathbf{C}^{-1} + a_4 \mathbf{Q}] : d\mathbf{C} \quad (58)$$

Taking advantage of the results provided by Simo and Taylor (1991), $d(\mathbf{n}^\alpha \otimes \mathbf{n}^\alpha)$ can be expressed as

$$d(\mathbf{n}^\alpha \otimes \mathbf{n}^\alpha) = \mathbf{W}^\alpha : \mathbf{T} : d\mathbf{C} \quad (59)$$

where the Cartesian components of \mathbf{T} are given by $T_{ijkl} = F_{ki}^{p,n,-1} F_{lj}^{p,n,-1}$ and where \mathbf{W}^α is a fourth-order tensor which can be expressed in terms of the eigenbasis $\mathbf{n}^\alpha \otimes \mathbf{n}^\alpha$ and the eigenvalues $\lambda^{e,tr,\alpha}$ (Simo and Taylor, 1991), for the explicit expressions of \mathbf{W}^α .

REFERENCES

- Andersson, H. (1977). Analysis of a Model for Void Growth and Coalescence Ahead of a Moving Crack Tip, *J. Mech. Phys. Solids*, **25**(3): 217–233.
- Aravas, N. (1987). On the Numerical Integration of a Class of Pressure-dependent Plasticity Models, *Int. J. Numer. Meth. Engng*, **24**(7): 1395–1416.
- Bažant, Z. and Lin, F. (1988). Non-local Yield Limit Degradation, *Int. J. Numer. Meth. Engng*, **26**(8): 1805–1823.
- Becker, R. and Needleman, A. (1986). Effect of Yield Surface Curvature on Necking and Failure in Porous Plastic Solids, *J. Appl. Mech.*, **53**(3): 491–499.
- Benzerger, A., Besson, J., Batisse, R. and Pineau, A. (2002). Synergistic Effects of Plastic Anisotropy and Void Coalescence on Fracture Mode in Plane Strain, *Modelling Simul. Mater. Sci. Eng.*, **10**(1): 73–102.
- Brown, L.M. and Embury, J.D. (1973). The Initiation and Growth of Voids at Second Phase Particles, In: *the Third International Conference on the Strength of Metals and Alloys, Vol. 1* Monograph and Report Series, **36**: 164–169, Institute of Metals, London, United Kingdom.
- Budiansky, B. (1970). Thermal and Thermoelastic Properties of Isotropic Composites, *J. Composite Materials*, **4**: 286–295.
- Davison, L. Stevens, A. and Kipp, M. (1977). Theory of Spall Damage Accumulation in Ductile Metals, *J. Mech. Phys. Solids*, **25**(1): 11–28.
- de Borst, R. and Mühlhaus, H. (1992). Gradient-dependent Plasticity: Formulation and Algorithmic Aspects, *Int. J. Numer. Meth. Engng*, **35**(3): 521–539.
- de Borst, R., Benallal, A. and Heeres, O. (1996). A Gradient Enhanced Damage Approach to Fracture, *J. Phys.*, **IV C6**: 491–502.
- Gurson, A. (1975). Plastic Flow and Fracture behavior of Ductile Materials Incorporating Void Nucleation, Growth, and Interaction, PhD Thesis, Brown University, Applied Mechanics.
- Gurson, A. (1977). Continuum Theory of Ductile Rupture by Void Nucleation and Growth: Part 1- Yield Criteria and Flow Rules for Porous Ductile Media, *J. Engng. Materials Technol.*, **99**(1): 2–15.
- Håkansson, P., Wallin, M. and Ristinmaa, M. (2006). Thermomechanical Response of Non-local Porous Material, *Int. J. Plast.*, **22**: 2066–2090.
- Hancock, J. and Mackenzie, A. (1976). On The Mechanisms of Ductile Failure in High-strength Steels Subjected to Multi-axial Stress-states, *J. Mech. Phys. Solids*, **24**(2): 147–169.
- Kachanov, L. (1958). Rupture Time Under Creep Conditions, *Izvestija Akademii Nauk SSSR, Otdelene Tekhnicheskich Nauk.* (In Russian) (English Translation: *Rupture Time Under Creep Conditions Int. J. Frac.* (97), pp. xi–xviii), **8**(1): 26–31.

- Kojic, M., Vlastelica, I. and Zikovic, M. (2002). Implicit Stress Integration Procedure for Small and Large Strains of the Gurson Model, *Int. J. Numer. Meth. Engng*, **53**(12): 2701–2720.
- Kröner, E. (1960). Allgemeine Kontinuumsmechanik der Versetzungen und Eigenspannungen, *Arch. Rational Mech. Anal*, **4**(4): 273–334.
- Lassance, D., Scheyvaerts, F. and Pardoën, T. (2006). Growth and Coalescence of Penny-shaped Voids in Metallic Alloys, *Engng. Fract. Mech.*, **73**(8): 1009–1034.
- Lee, E.H. (1969). Elastic-plastic Deformation at Finite Strains, *J. Appl. Mech.*, **36**(1): 1–6.
- Lemaitre, J. and Chaboche, J.-L. (1990). *Mechanics of Solid Materials*, Cambridge University Press, Cambridge, United Kingdom, English edition.
- Mahnken, R. (1999). Aspects of the Finite-element Implementation of the Gurson Model Including Parameter Identification, *Int. J. Plasticity*, **15**(11): 1111–1137.
- Mahnken, R. (2002). Theoretical, Numerical and Identification Aspects of a New Model Class for Ductile Damage, *Int. J. Plasticity*, **18**(7): 801–831.
- Menzel, A., Ekh, M., Runesson, K. and Steinmann, P. (2005). A framework for Multiplicative Elastoplasticity With Kinematic Hardening Coupled to Anisotropic Damage, *Int. J. Plasticity*, **21**(3): 397–434.
- Miehe, C. (1998). Comparison of two Algorithms for the Computation of Fourth Order Isotropic Tensor Functions, *Comp. Struct.*, **66**(1): 37–43.
- Mühlich, U. and Brocks, W. (2003). On the Numerical Integration of a Class of Pressures-dependent Plasticity Models Including Kinematic Hardening, *Comp. Mech.*, **31**(6): 479–488.
- Needleman, A. and Rice, J. (1978). Limits to Ductility Set by Plastic Flow Localization, In: Kostinen, D.P. et al. (eds), *Mechanics of Sheet Metal Forming*, pp. 237–267, Plenum Publishing Corporation.
- Olsson, M. (2003). Plasticity Driven Damage and Void Growth, PhD Thesis, Dep. Mech. Engng., Solid Mechanics, Lund University, Sweden.
- Olsson, M. and Ristinmaa, M. (2003). Damage Evolution in Elasto-plastic Materials – Material Response due to Different Concepts, *Int. J. Damage Mechanics*, **12**(2): 115–139.
- Ottosen, N. and Ristinmaa, M. (2005). *The Mechanics of Constitutive Modeling*, Elsevier, First edition.
- Rabier, P. (1989). Some Remarks on Damage Theory, *Int. J. Engng. Sci.*, **27**(1): 29–54.
- Rousselier, G. (1987). Ductile Fracture Models and their Potential in Local Approach of Fracture, *Nucl. Engng and Des.*, **105**(1): 97–111.
- Simo, J.C. and Miehe, C. (1992). Associative Coupled Thermoelasticity at Finite Strains: Formulation, Numerical Analysis and Implementation, *Comput. Methods Appl. Mech. Engng*, **98**(1): 41–104.
- Simo, J.C. and Taylor, R.L. (1991). Quasi-incompressible Finite Elasticity in Principle Stretches. Continuum Basis and Numerical Algorithms, *Comput. Methods Appl. Mech. Engng*, **85**(3): 273–310.
- Springmann, M. and Kuna, M. (2005). Identification of Material Parameters of the Experimental and Numerical Techniques, *Computational Materials Science*, **32**(3): 544–552.
- Strömberg, L. and Ristinmaa, M. (1996). FE-formulation of a Nonlocal Plasticity Theory, *Comput. Methods Appl. Mech. Eng.*, **136**(1): 127–144.
- Svedberg, T. and Runesson, K. (1997). A Thermodynamically Consistent Theory of Gradient-regularised Plasticity Coupled to Damage, *Int. J. Plasticity*, **13**(6): 669–696.
- Truesdell, C. and Toupin, R.A. (1960). The Classical Field Theories, In: Flugge, S. (ed.), *Handbuch der Physik*, Vol. III/1, pp. 226–793, Springer-Verlag, Berlin, Germany.
- Tvergaard, V. (1981). Influence of Voids on Shear Band Instabilities Under Plane Strain Conditions, *Int. J. Fracture*, **17**(4): 389–407.

- Tvergaard, V. and Needleman, A. (1984). Analysis of the Cup-cone Fracture in a Round Tensile Bar, *Acta Metall*, **32**(1): 157–169.
- Wang, D.A., Pan, J. and Liu S.D. (2004). An Anisotropic Gurson Yield Criterion for Porous Ductile Sheet Metals with Planar Anisotropy, *Int. J. Damage Mechanics*, **13**(1): 7–33.
- Wallin, M. and Ristinmaa, M. (2001). Accurate Stress Updating Algorithm Based on Constant Strain Rate Assumption, *Comput. Methods Appl. Mech. Eng.*, **190**(42): 5583–5601.
- Weber, G. and Anand, L. (1990). Finite Deformation Constitutive Equations and a Time Integration Procedure for Isotropic, Hyperelastic-viscoplastic Solids, *Comput. Methods Appl. Mech. Eng.*, **79**(2): 173–202.
- Wriggers, P., Miehe, C., Klieber, M. and Simo, J. (1992). On the Coupled Thermomechanical Treatment of Necking Problems via Finite Element Methods, *Int. J. Numer. Meth. Eng.*, **33**(7): 869–883.